Bull. Chem. Soc. Jpn., **78**, 1373–1383 (2005)

Award Accounts

The Chemical Society of Japan Award for Creative Work for 2003

Design of Functional Molecular Crystals by Controlling Intermolecular Interactions

Tamotsu Inabe

Division of Chemistry, Graduate School of Science, Hokkaido University, Sapporo 060-0810

Received January 28, 2005; E-mail: inabe@sci.hokudai.ac.jp

In this account, two representative approaches toward the control of molecular arrangements in molecular crystals are introduced, especially for π-radicals. One is "π–π stacking structure modification of macrocyclic π-ligand complexes", in which the interaction is modified by simply introducing axial ligands. By this method, a number of conductors with various π–π stacking structures have been obtained. The other is "design of functional crystals utilizing hydrogen bonds", in which anions with strong self-assembling ability are used for the formation of anion networks. If the interaction between the anions is stronger than that between π-radical cations, the cations are expected to be packed in the space provided by the networks with peculiar assembly formations that differ from those inherently preferable for the cations. The arrangement of π-radicals is directly related to the electronic functionalities of the crystal, and its control is crucial for the design of the specific electronic functionalities.

1. Introduction and Outline of This Study

The physical properties and functionalities of molecular crystals can be designed through the design of the constituent "molecule". Especially when the constituent is a π-radical, it is important to control the packing in the crystal because the charge transport and magnetic interactions are dominated by the relative arrangement of the radicals. Electronic stabilization will be attained by overlapping the orbitals which accommodate an unpaired electron, causing attractive interactions between π-radicals. Also, in molecular conductors, this orbital overlap produces the conduction paths, and the stabilized structure itself contributes to the specific charge transport properties. Therefore, in the design of molecular conductors, it has been considered to be undesirable to disturb the arrangements preferable for the open-shell molecules.

However, this guideline will limit the arrangements into a narrow range of structures in which given π-radicals are spontaneously arranged. As mentioned above, it is necessary to control the relative arrangement to some extent for the control or design of physical properties. From this point of view, we have intended to design some molecular crystals according to our proposal of "imposing frustrated relative arrangements".

The first method is simply to disturb the preferred arrangements by steric effects. In this study, a macrocyclic π-ligand of phthalocyanine was adopted as the π-radical part, and steric hindrance was introduced by attaching axial ligands at the central metal ion. Phthalocyanines (Scheme 1) have been known to give conductors by oxidizing the π-ligand to make it an open-shell structure since 1980.[1] These conductors were composed of planar M(Pc)s (Pc = phthalocyaninato) with divalent metals. The composition is M(Pc)X$_y$ ($1/3 \leq y \leq 1/2$), and it may be characterized by a one-dimensional columnar structure that is advantageous to maximize the overlaps between π-HOMO's. This interaction is significant, and the same structural motif appears for the various anions (X = I_3^-, BF_4^-, AsF_6^-, SbF_6^-, Br_3^-). Though their electrical conductivities were high and some maintain the high conductivity at low temperature, it was necessary to increase the dimensionality of the electronic system in order to make them superconductors. Then, we challenged this subject by utilizing axially substituted phthalocyanines to disturb the preferred columnar structure. As a result, a series of conductors with various dimensionalities of stacking structures have successfully been developed, and this work is described in section **2**.

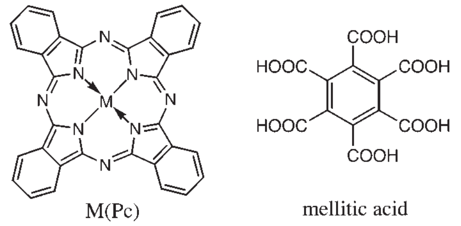

Scheme 1.

The second method was proposed based on hydrogen bonds of which the energy is comparable to that of π–π interactions between radicals. The energy of the interactions operating be-

Published on the web August 4, 2005; DOI 10.1246/bcsj.78.1373

tween open-shell π-conjugated molecules is rather strong (0.1–0.3 eV) with strong directionality due to the necessity of overlapping the orbitals. Similarly, hydrogen bonds possess comparable energy of bonding and directionality. However, if there is only a single hydrogen bond between molecules, it may not be strong enough to regulate the molecular arrangement. Therefore, it may be desirable that there are two or more intermolecular hydrogen bonds. One could design π-radical molecules that have hydrogen-bonding functional groups. In this case, however, the synthesis may be difficult, and the variation of the resultant structures may be restricted within some narrow range. A wide variety of the structures can be produced in the design of two-component materials in which one component forms a network and the other π-radical component is packed in/between the networks. As an example of such a component, we investigated the networks of mellitate that is produced by partial deprotonation of mellitic acid (benzene hexacarboxylic acid; Scheme 1). When mellitate was combined with π-radical cations, the anion formed channel structures or sheet structures depending on the cationic species. The resultant π-radical arrangements were found to be considerably different from the spontaneously formed assembly structures of the radicals. These examples are described in section **3**. The details of the mellitate networks may be found in the recent review.[2]

2. Molecular Arrangement Control and Electronic Functionalities in Crystals Composed of Macrocyclic π-Ligand Complexes

2.1 One-Dimension to Two-Dimension. After the discovery of phthalocyanine-based conductors at Northwestern University in the beginning of the 1980s, their chemical and physical properties were actively studied by mainly two groups in the same university.[1] The objects included not only M(Pc)X$_y$-type molecular conductors but also the oxygen-bridged [M(Pc)O]$_n$ polymers.[3] Both of them have a one-dimensional columnar structure, and holes generated in the π-ligand by partial oxidation are transported in this column. Most of the molecular conductors showed clear metallic behaviors.

In the meantime, the first organic superconductor based on TMTSF (tetramethylfulvalene) was discovered,[4] and superconductivity became an attractive subject of molecular conductors. Shortly after, several superconductors based on BEDT-TTF (bis(ethylenedithia)tetrathiafulvalene) were successively discovered, and it was recognized that the two-dimensionality of the electronic system is crucial for achieving the superconducting state.[5] In TMTSF and BEDT-TTF, selenium or sulfur atoms included in the π-conjugate system made it possible for these donors to overlap the π-orbital with those in the neighboring molecules along the directions parallel to the molecular plane. This expanded the conduction path that had been restricted in the one-dimensional π–π stacking column into the transverse directions, and made it possible to realize the stable metallic and superconducting ground states.

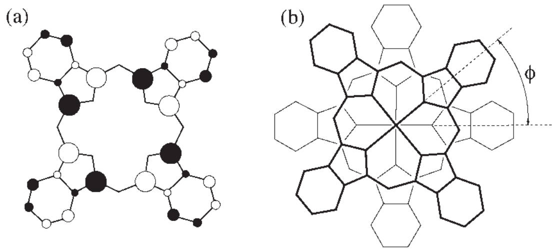

Fig. 1. (a) Schematic representation of the HOMO coefficients of the Pc ligand. (b) Staggering angle (ϕ) in the metal-over-metal type Pc column.

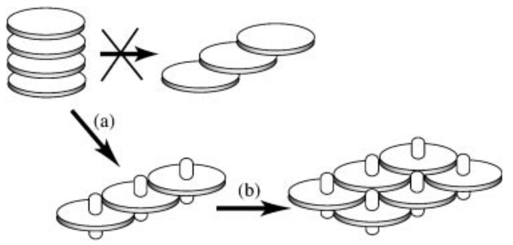

Fig. 2. Schematic representation of the Pc ligand stacking. (a) Slipped stacking induced by axial substitution. (b) Two-dimensional stacking by additional overlaps between the one-dimensional stacks.

Compared with the above systems, the Pc conductors were highly one-dimensional. Indeed, the systematic comparison of M(Pc)X$_y$ and {[M(Pc)O]X$_y$}$_n$ revealed that their physical properties were dominated only by the π–π interaction within the column (interplanar spacing).[3] In the Pc system, the HOMO–HOMO interaction between the Pc ligands is important, since the oxidation occurs in the Pc π-system. The most efficient overlap occurs when M(Pc)s' stack in a metal-over-metal fashion and the neighboring rings form a rotation angle (ϕ) of 0 or 45°,[6] as shown in Fig. 1. In the real structures, the eclipsed stacking of $\phi = 0°$ was not favorable due to the atom–atom repulsion, and the staggered stacking with ϕ of nearly 40° was always observed. The overlap integral at $\phi = 40°$ is large, and the metal-over-metal stacking is exclusively dominant because the transverse shifting of the rings always reduces the value. If one could impose the slipped stack structure shown in Fig. 2, higher dimensionality of the electronic system would be realized. However, in this case, the fear that such a partial overlap is not efficient enough for the conduction path would arise. This point was positively supported by the following two experimental data. One was involved in the study of a pyrazine bridged polymer, [Fe(Pc)(pyz)]$_n$, developed by Hanack. This polymer has a considerably longer interplanar spacing (about 6.8 Å) compared with the oxygen-bridged Pc polymers. However, the iodine doping resulted in high conductivity which was comparable with that of {[Ge(Pc)O]I}$_n$ (interplanar spacing of 3.48 Å).[7] This suggested that the π–π stacking interaction became possible by inserting the Pc planes between the neighboring polymer chains. The other came from the doping of Ga(Pc)Cl; a Pc molecule that could not form a face-to-face stacked one-dimensional column. The BF_4^--doped powder showed high conductivity of 10^{-1} S cm^{-1}.[8] In both cases, the Pc rings are stacked only partially due to the axial substituent of pyrazine or chloride. Their high conductivity suggested that the conduction path could be formed for such a slipped structure.

These facts encouraged us in designing conducting crystals by using axially substituted Pc molecules. Then, we attempted to grow partially oxidized crystals of Al(Pc)Cl and Ga(Pc)Cl. However, we failed to grow the crystals and to study the details of the structural and physical properties due to the poor solubility of the component Pc molecules.

2.2 Highly Soluble [M(Pc)(CN)$_2$]$^-$. During the above research, it was reported in 1985 by a group at Waseda University that electrolysis of K[Co^{III}(Pc)(CN)$_2$] yielded highly conducting crystals.[9] The parent salt was synthesized by Hanack's group as a precursor of the CN-bridged Pc polymer.[10] This salt was dissolved in acetonitrile, and an electric field applied to this solution yielded conducting crystals on the anode surfaces. The room temperature conductivity was as high as about 50 S cm^{-1}. Strangely, the structure analysis was failed, and they proposed a model of this crystal in which one of the axial CN groups was eliminated and the neutral Co^{III}(Pc)(CN) units formed conduction paths of slipped π-ligand stacking. This model was thought to be suspicious, since the origin of the charge carrier was unclear and d^6 Co^{III} had to take an unnatural penta-coordination. The structure was left unsolved for several years, so we decided to prepare this crystal. K[Co^{III}(Pc)(CN)$_2$] was prepared following the method reported by Hanack, and we noticed its surprisingly high solubility compared with other peripheral unsubstituted Pc compounds. The salt is soluble in ordinary solvents such as acetone, acetonitrile, and alcohols, and is soluble even in water though the solubility is not high. The crystal growth was performed without adding electrolytes because the starting material is a salt. The crystals obtained on the anode surfaces in the acetonitrile solution were found to have the sufficient size for X-ray structure analysis. However, when the crystals were once taken out from the solution, the diffraction peaks were not observable. This phenomenon frequently occurred when the crystal contained a crystal solvent, and indeed, the diffraction peaks were clearly observed when the crystal was sealed in a glass capillary with the mother liquor. The structure analysis indicated that this electrolysis product was a cation deficient partially oxidized salt containing a large number of solvent molecules; K[Co^{III}(Pc)(CN)$_2$]$_2\cdot$5CH$_3$CN.[11] As shown in Fig. 3, some of CH$_3$CN molecules are packed in the open space without any interactions with the surroundings, and these are supposed to immediately come out from the crystal when it is taken out from the solution. The Pc rings are slipped a large distance due to the axial ligands, forming a two-dimensional π–π stacking sheet. From the cation to anion ratio, each Pc ring is formally oxidized by 0.5e. Its high conductivity even for the mosaic crystal indicated that a sufficient conduction path would be formed by stacking only the peripheries of the Pc rings.

Since this crystal was so unstable, the properties could not be examined in detail. However, it became clear that the conducting crystals could be designed by replacing some components in this crystal. Also it was found that the [Co^{III}(Pc)(CN)$_2$]$^-$ anion had high solubility suitable for crystal growth. We started the study on the crystal design and crystal growth by using this anion in 1994.

2.3 Neutral Radical Crystals. In the early study, crystal growth using the potassium salt was performed in various solvents in order to replace CH$_3$CN in the model K[Co^{III}(Pc)(CN)$_2$]$_2\cdot$5CH$_3$CN crystal with other solvent molecules. As a result, several crystals were obtained. However, they were found to be the neutral radical crystals that do not contain any cations.[12,13] The neutral radical crystallized with various solvent molecules, and the π–π stacking structure was found to vary by the solvent species in the lattice. The neutral radical crystal with one-dimensional π–π stacking structure contained CHBr$_3$ as the crystal solvent (Fig. 4a), and those with two-dimensional stacking structure (Fig. 4b) contained CHCl$_3$, DMSO, or the like. When the crystal solvent was more com-

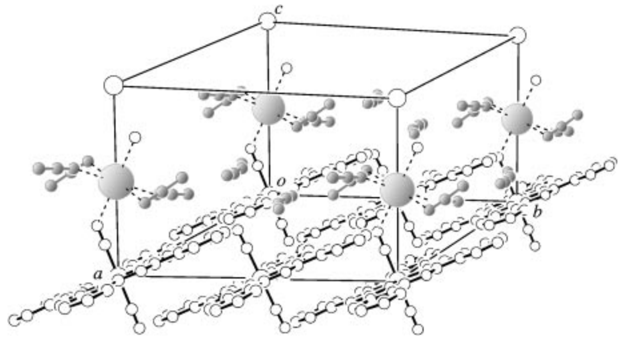

Fig. 3. Crystal structure of K[Co^{III}(Pc)(CN)$_2$]$_2\cdot$5CH$_3$CN. The larger gray spheres are potassium ions and molecules with smaller gray spheres are acetonitrile. Acetonitrile molecules that do not coordinate to potassium are disordered.

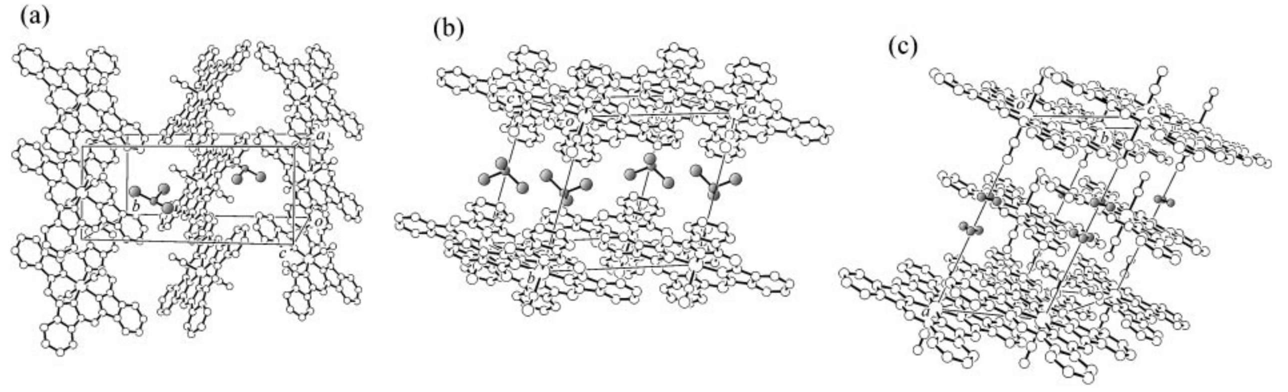

Fig. 4. Structures of the [Co^{III}(Pc)(CN)$_2$] neutral radical crystals. (a) CHBr$_3$ inclusive crystal with one-dimensional π–π stacking. (b) CHCl$_3$ inclusive crystal with two-dimensional π–π stacking. (c) H$_2$O inclusive crystal with one-dimensional π–π stacking.

pact H_2O, further π–π interaction between the two-dimensional sheets became possible, and the total π–π stacking interaction became three-dimensional (Fig. 4c). However, introduction of H_2O into the crystal-growth system was not desirable to grow large crystals of $[Co(Pc)(CN)_2]\cdot 2H_2O$, because the CN-bridged polymer was known to form in the aqueous suspension of $[Co(Pc)(CN)_2]^-$.[10] In some conditions, the solvent-free crystal of $[Co(Pc)(CN)_2]$ could be obtained.[13] In this crystal, the π-ligands of the neighboring Pc units were not parallel to each other, and the π–π interaction could be regarded to be discrete (zero-dimensional).

Li(Pc) and $Lu(Pc)_2$ are famous as the Pc-based neutral radicals.[14,15] Their room temperature conductivity (about 10^{-3} $S\,cm^{-1}$) is, however, only comparable to that of the worst conductor of solvent-free $[Co(Pc)(CN)_2]$. The solvent-inclusive crystals showed much higher conductivity; especially, $[Co(Pc)(CN)_2]\cdot 2H_2O$ with three-dimensional π–π interactions showed 1 $S\,cm^{-1}$ even for the powder compaction sample. Li(Pc) crystallized in a face-to-face stacked column similar to $M(Pc)X_y$-type partially oxidized salts.[16] Higher conductivities of the $[Co(Pc)(CN)_2]$-based neutral radical crystals suggested that the sufficient conduction path was formed even when the π–π stacking of the Pc rings was only partial. Also, this study indicated that it might be possible to construct multi-dimensional π–π stacking structure by varying the second crystal component.

For the π-extended system, $[Co(2,3\text{-nc})(CN)_2]$ (2,3-nc = 2,3-naphthalocyaninato), the neutral radical crystals were also obtained.[17] In these cases, the extended π-system made it possible to maintain multi-dimensional π–π stacking interaction even for large crystal solvents, and high conductivity values were observed. In order to increase the π–π interaction in the neutral radical crystals, we applied pressure on $[Co(2,3\text{-nc})(CN)_2]\cdot CH_3CN$, in which three-dimensional π–π stacking interaction was achieved. The conductivity was increased successively with pressure; however, the metallic state was not observed yet.[18]

2.4 Partially Oxidized Salt Crystals. Since the above approach to obtaining the stable partially oxidized salts by replacing the crystal solvent species of $K[Co^{III}(Pc)(CN)_2]_2\cdot 5CH_3CN$ exclusively gave the neutral radical crystals, we then attempted to grow the partially oxidized salt crystals by replacing the "cation and solvents" part with organic cations. In the early stage, various cationic species with somewhat large size were adopted; however, the neutral radical crystals were dominated in all cases.

This situation was improved by finding beautiful needle crystals on the anode of electrolysis of the TPP (TPP = tetraphenylphosphonium; Scheme 2) salt.[19] The room temperature conductivity was 120 $S\,cm^{-1}$, a value that was more than two orders higher than that of the best neutral radical conductor, suggesting its partially oxidized state. Though the shape was largely different from M(Pc) due to the addition of axial ligands to differentiate the stacking structure, the resultant crystal system was tetragonal, like that of $M(Pc)X_y$-type conductors, and the π–π stacking occurred only along the one direction (Fig. 5). The composition, $TPP[Co(Pc)(CN)_2]_2$, indicated that the Pc ligand is formally oxidized by 0.5e. Since the one-dimensional chain was completely uniform (the repeat unit of the π–π stacking coincides with the unit *c*-length), the energy band composed of HOMO of the Pc ligand was suggested to be a 3/4-filled metallic band. Indeed, the thermoelectric power showed metallic behavior above 100 K, and the estimated band width of 0.5 eV was in good agreement with that estimated by optical reflectance spectra. However, the temperature dependence of the electrical conductivity was not clearly metallic; the value was almost constant around room temperature and decreased with lowering temperature with an apparently small thermal activation energy. This behavior was thought to be mainly due to the narrow band width, a characteristic of this system, and this behavior became more pronounced in the systems with narrower band widths; the overlap integral (proportional to the band width) decreased in the order of $TPP[Co(Pc)(CN)_2]_2$, $TPP[Co(Pc)Br_2]_2$, and $TPP[Co(1,2\text{-Nc})(CN)_2]_2$ (1,2-Nc = 1,2-naphthalocyaninato), and the conduc-

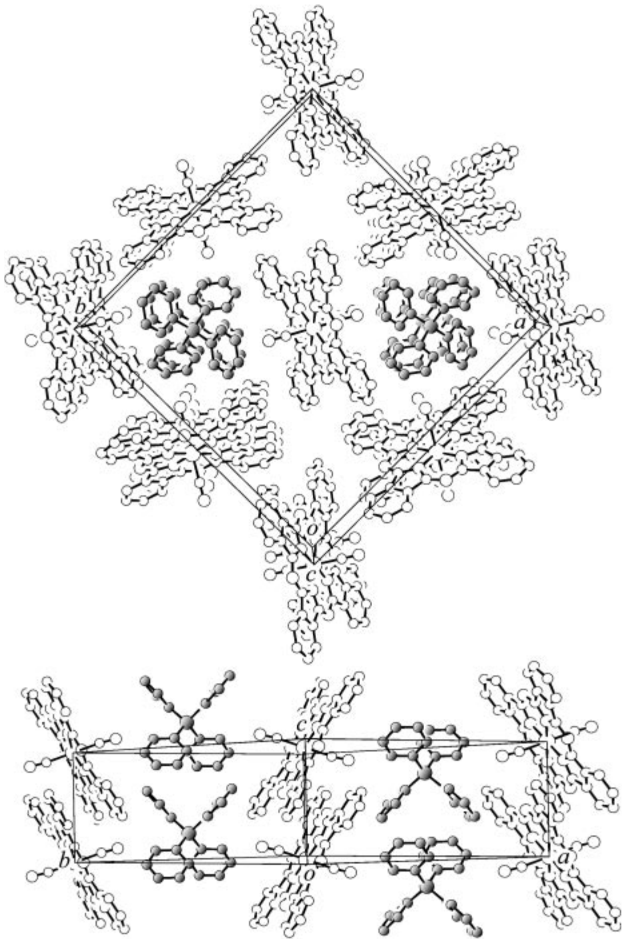

Fig. 5. Crystal structure of the partially oxidized $TPP[Co^{III}(Pc)(CN)_2]_2$.

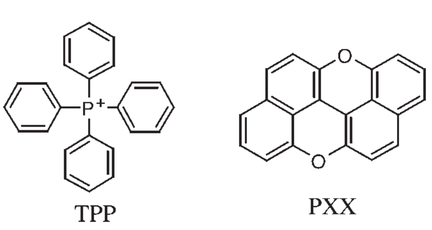

Scheme 2.

tivity decrease and apparent activation energy increase were observed following this order.[20] A similar partially oxidized one-dimensional system was obtained by combining with PTMA (PTMA = phenyltrimethylammonium).[21] In this case, the number of the cationic sites was 1:1 to number of the Pc sites. However, the cationic sites were randomly occupied by acetone or acetonitrile, and the composition became $[\mathrm{PTMA}]_x[\mathrm{Co(Pc)(CN)}]\cdot y(\mathrm{solvent})$. Its physical properties were nearly identical with those of the TPP salt: metallic thermoelectric power above 100 K and thermally activated conductivity below 250 K.

In the combination with closed-shell cations, the partially oxidized salts were so far obtained only for the above two cations, and both were unexpectedly one-dimensional. Then, we changed the cationic species to those with open-shell structures. For the crystal growth of closed-shell cations, once the cation exchange of the potassium salt was done, then electrolysis of the salt was performed. For open-shell cations with high solubility, the same procedure was applied, and the 1:1 salts of $[\mathrm{Co^{III}(Pc)(CN)_2}]^-$ with α-nitronyl nitroxide pyridiniums were obtained.[22] Though their magnetic properties were measured, construction of the partially oxidized salts did not succeed. Another method may be to use donor molecules that give radical cations by electrochemical oxidation. In this case, the electrolysis of the solution containing both a salt of $[\mathrm{Co(Pc)(CN)_2}]^-$ and a neutral donor (D) might give salts in which both components are oxidized, and the composition could be $[\mathrm{D}_x]^{\delta+}[\mathrm{Co(Pc)(CN)_2}]^{\delta-}$. For the crystal growth with TTF (tetrathiafulvalene) and TMTTF (tetramethyltetrathiafulvalene), the salts with $x = 1$ and $\delta = 1$ were obtained, and the Pc ligand was not oxidized.[23] A unique salt was obtained by the combination with benzo[c]phenothiazine (B[c]PT), in which the CN-bridged dimeric Pc unit was found as $[\mathrm{B[c]PT}]^+[\mathrm{(CN)Co(Pc)–CN–Co(Pc)(CN)}]^-$.[24] This observation suggests that the following equilibrium exists in the solution;

$$2[\mathrm{Co(Pc)(CN)_2}]^- \rightleftharpoons [\mathrm{(CN)Co(Pc)–CN–Co(Pc)(CN)}]^- + \mathrm{CN}^-. \tag{1}$$

In this case, the Pc ligand was again not oxidized. These donors commonly have relatively low oxidation potentials, and the difference from that of the $[\mathrm{Co(Pc)(CN)_2}]^-$ unit (ca. 1 V vs $\mathrm{Ag/Ag^+}$ in acetonitrile) is rather large. On the other hand, the combination with a donor, PXX (*peri*-xanthenoxanthene or 6,12-dioxaanthanthrene; Scheme 2), with a relatively high oxidation potential (ca. 0.8 V) was found to give two kinds of needle crystals with $x = 1$ and $\delta = 1/2$ and with $x = 2$ and $\delta = 1/2$.[15,16] In both crystals, the Pc ligand was in a partially oxidized state, and it was found that the redox potentials had to be close to each other for obtaining the partially oxidized salts. This relation is somewhat similar to that found in the donor–acceptor combination.[25]

In the crystal with $x = 1$ and $\delta = 1/2$, $[\mathrm{PXX}][\mathrm{Co(Pc)(CN)_2}]$, both components are in the partially oxidized states. As shown in Fig. 6, in this crystal, PXX forms a one-dimensional column with a two-fold repeat unit, while the Pc unit forms a one-dimensional chain with a single repeat unit. Furthermore, there is a meaningful π–π interaction between the two chains, forming a ladder chain.[26]

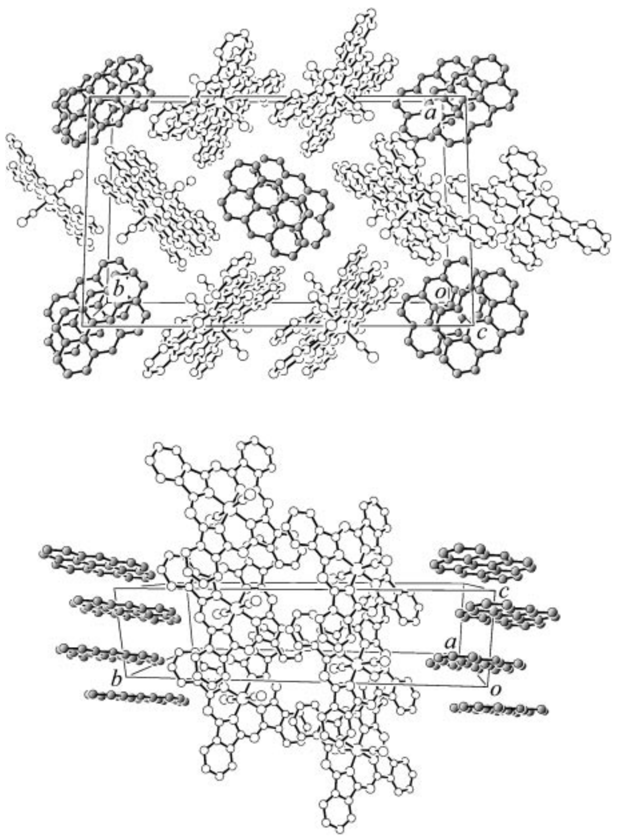

Fig. 6. Crystal structure of $[\mathrm{PXX}][\mathrm{Co^{III}(Pc)(CN)_2}]$.

On the other hand, in the crystal with $x = 2$, $\delta = 1/2$, $[\mathrm{PXX}]_2[\mathrm{Co(Pc)(CN)_2}]$, the formal charge of the Pc ligand is the same as that in the above crystal, whereas that of PXX reduces to $+1/4$. PXX forms again a one-dimensional column with a two-fold repeat unit in this crystal (Fig. 7). The Pc unit forms a uniform one-dimensional chain along the *c* axis, and in this crystal the neighboring chains interact infinitely by π–π stacking interactions.[27]

The temperature dependence of the conductivity along the needle axis in these crystals is shown in Fig. 8 with that in the previous single chain partially oxidized salt. There could be some contribution from the partially oxidized one-dimensional PXX columns. However, the two-fold periodicity makes the band width extremely narrow, and the contribution must be negligibly small. In all the cases, therefore, the conductivity behavior must be dominated by the uniform conduction paths formed by the Pc π-systems. Compared with the obscure temperature dependence in the single chain conductor, the metallic behavior is clear in the ladder chain conductor above 100 K. In the 2D sheet conductor, the room temperature value increases one order; here the metallic behavior is further pronounced. Though the conductivity gradually decreases below 100 K, it retains high values comparable to the room-temperature value even at 5 K. Since the HOMO–HOMO overlap integral value along the needle axis is nearly the same for the three crystals, the increased conductivity with clear metallic behavior in the 2D sheet conductor is thought to result from the participation of the transverse π–π interactions. However, the π–π interaction in the 2D Pc sheet is still largely anisotropic, and the electronic system is not truly two-dimensional. Indeed, the optical

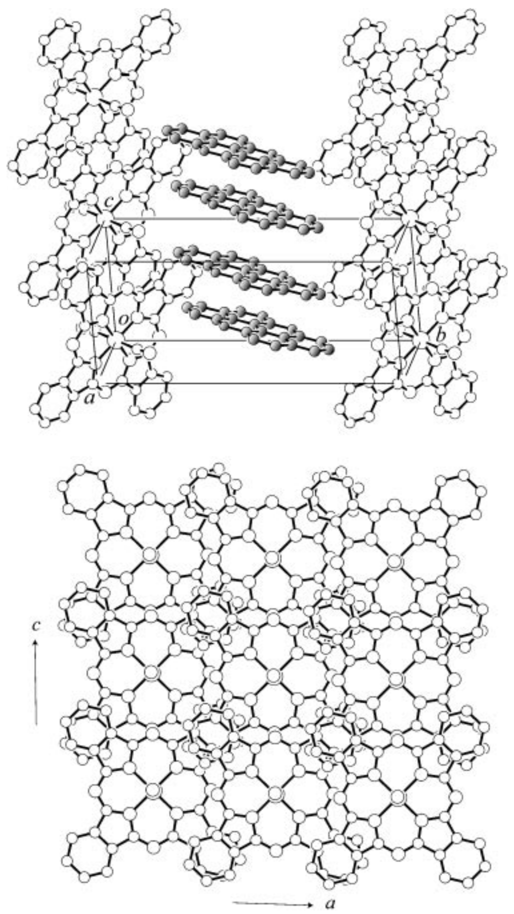

Fig. 7. Crystal structure of $[PXX]_2[Co^{III}(Pc)(CN)_2]$.

reflectance spectra showed the dispersion only along the *c* axis, indicating its quasi-one-dimensional electronic structure.

In combination with PXX, platelet crystals were also obtained besides these two needles. In these crystals, more isotropic two-dimensional π–π interactions have been noticed. Further study on their structures and physical properties is now in progress.

2.5 Introduction of Magnetic Moments. In the above study, the central metal of the Pc system was always Co^{III}. The low-spin d^6 configuration by the strong octahedral ligand field makes this ion non-magnetic. This situation is convenient for examining the physical properties originating from the pure π-electron systems. However, if one could introduce a magnetic central metal ion, a unique π–d system composed of π-centered conduction electrons and d-centered magnetic moments would be constructed. Since the geometrical conformation of macrocyclic π-ligands such as phthalocyanines is rather insensitive to the central metal species, it is expected that isostructural crystals can be obtained for M^{III} other than Co^{III}. Then, as the simplest replacement, the Fe^{III} system in which the low-spin d^5 configuration gave $S = 1/2$ was investigated.

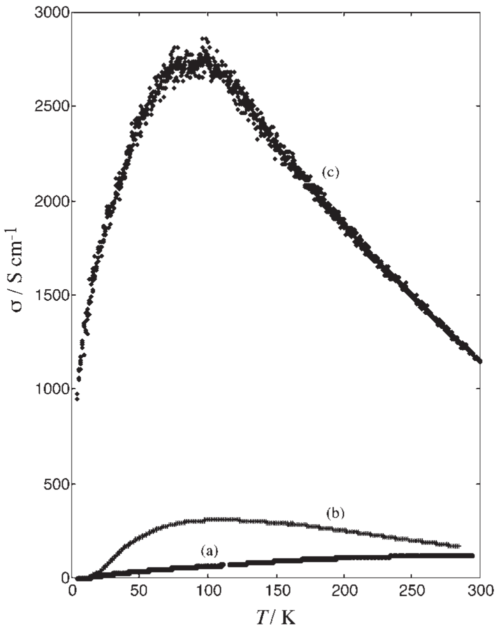

Fig. 8. Temperature dependence of the electrical conductivity of (a) $TPP[Co^{III}(Pc)(CN)_2]_2$, (b) $[PXX][Co^{III}(Pc)(CN)_2]$, and (c) $[PXX]_2[Co^{III}(Pc)(CN)_2]$.

Three kinds of the partially oxidized salts, $TPP[Fe(Pc)(CN)_2]_2$, $[PTMA]_x[Fe(Pc)(CN)_2]\cdot y(\text{solvent})$, and $[PXX][Fe(Pc)(CN)_2]$, which had isomorphous structures with the Co^{III} system were obtained, and their properties were examined.[21,28,29] Firstly, the HOMO–HOMO overlap integrals estimated from their structural data were compared, and it was found that the values were not so much different from those in the Co^{III} system. This indicated that the π–π interactions were not affected by the central metal species, and in fact the reflectance spectra and thermoelectric power above 100 K were almost the same for the Co^{III} and the Fe^{III} systems. However, the temperature dependence of the thermoelectric power at low temperature in the Fe^{III} system showed significantly larger deviations from the metallic behavior than those found in the Co^{III} system. Furthermore, the electrical resistivity in the Fe^{III} system increased rapidly at low temperature, and the difference from the Co^{III} system became more than several orders around 20 K. This was thought to be due to the effects of the localized magnetic moments in the Fe^{III} system; conduction electrons were subjected to extra scattering compared with the Co^{III} system. Since this scattering could be suppressed by the external magnetic field, Hanasaki et al. measured the magnetoresistance.[30] As a result, the giant negative magnetoresistance was observed below about 40 K. This magnetoresistance was largely anisotropic, and the anisotropy was found to have correlation with the anisotropy of the magnetic susceptibility. From the ESR measurements of the $[Fe^{III}(Pc)(CN)_2]^-$ salt, it was found that the $Fe^{III}(Pc)(CN)_2$ unit itself has a largely anisotropic *g*-tensor, and it became clear that the larger negative magnetoresistance was observed when the magnetic field was perpendicular to the Pc plane.[31] This system was proved to be a unique π–d system in which π-centered conduction electrons were coupled with the magnetic moments of Fe^{III} embedded in the π-ligand. This system also showed some interesting phenomena such as the existence of antiferromagnetic interactions that were thought to be mediated by π-conduction electrons and spontaneous magnetization at very low temperature. The details of the mechanisms of such phenomena are still unknown, and this system may be a good candidate for the detailed study of the π–d interactions.

3. Design of Functional Crystals Utilizing Hydrogen Bonds

3.1 Functionalities of Hydrogen Bonds. Hydrogen bonds are a fundamental building unit not only in biological systems but also in various organized functional assemblies. In addition to the function that connects two units, hydrogen bonds may also act as an electronic functional group by reversible proton transfer. The chromism of *N*-salicylideneanilines is a representative example of such coupling between the π-electron system and the intramolecular proton transfer function in the crystalline state. We have been studying how this chromic function would be affected by chemical modifications and intermolecular interactions.[32–37] This phenomenon is thought to be the simplest chemical reaction that can occur in the crystalline state, and, if one could combine this with crystalline electronic properties, novel molecular devices would be realized.

Another important function of hydrogen bonds is the ability of arranging molecules with large association energy and strong directionality. A single O–H···O hydrogen bond with the O···O distance of about 2.7 Å possesses bonding energy of about 20 kJ mol^{-1}, and this energy is comparable to that yielded by overlapping the π-orbitals between π-radicals. If there are several hydrogen bonds between the units, the association energy exceeds the π–π interaction between the radicals. In the situation where these two intermolecular interactions compete, arrangements by hydrogen bonds may dominate. From this point of view, a study on the control of π-radical arrangement by self-organized assembly by hydrogen bonds has been performed.

3.2 Mellitate Anion and Supramolecular Networks. As mentioned in the introduction, it may not be clever to design molecules with several hydrogen-bonding functional groups in a single π-radical because of difficulty of synthesis and inflexibility of crystal design. Then, we picked out mellitate as an anion that possesses several hydrogen-bonding functional groups. Each of the six carboxy groups in the parent mellitic acid can independently be deprotonated, and the resultant carboxylate group is also a hydrogen-bonding functional group. Since these groups are radially arranged around the central benzene core, the anion can form several hydrogen bonds between the neighbors. This will lead to the formation of infinite networks. This anion bears two unique features: the number of sites deprotonated (n of $[C_6(COO)_6H_{6-n}]^{n-}$; equal to the anionic negative charge) and the network patterns formed by self-assembly.

In order to examine how the anion networks are preferentially formed and how many variations of the structure occur, we have targeted the combinations with pyridiniums for the structural study.[38] Since such combinations contain both proton-donating carboxy and pyridinium-N$^+$H groups and proton-accepting carboxy, carboxylate, and pyridine-N groups, it may be possible to examine whether hydrogen bonds between mellitates always take priority or not. As a result, it was found that the mellitate networks were preferentially formed and that the network structures could be roughly classified into three groups. These network structures were also found in the other ammonium salts.[39] The outlines are given below.

3.2.1 Two-Dimensional Sheet: One of the typical structures was repeatedly observed for the anion with $n = 3$. As an example, the structure of the anion sheet in the 3-aminopyridinium salt, $[3\text{-}NH_2C_5H_4NH^+]_3\{[C_6(COO)_6H_3]^{3-}\}$ is shown in Fig. 9.[38] The arrangement of the anions is nearly hexagonal, and all the six functional groups participate in the hydrogen bonds with the neighboring anions. This arrangement is identical to that in the parent mellitic acid crystal, and all the carboxy–carboxy paired hydrogen bonds in the acid crystal are replaced by the carboxy–carboxylate single hydrogen bonds in the salt crystal (Scheme 3). This arrangement is possible for all the three deprotonation patterns, and the same sheet structure was observed for the piperidinium salt, $[C_5H_{10}NH_2{}^+]_3$-

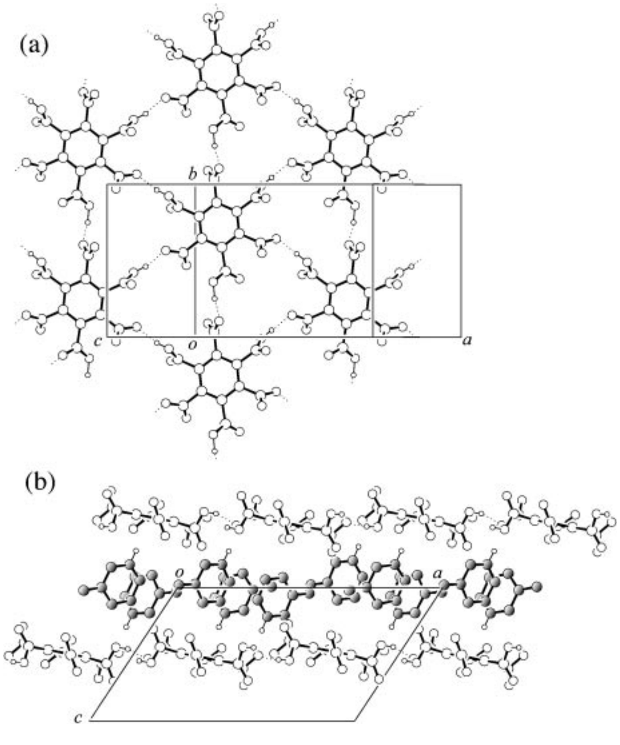

Fig. 9. Crystal structure of $[3\text{-}NH_2C_5H_4NH^+]_3\{[C_6(COO)_6H_3]^{3-}\}$. (a) Two-dimensional network of mellitate ($n = 3$). (b) Cation packing between the two-dimensional anion sheets. Fragments with gray spheres are the cations.

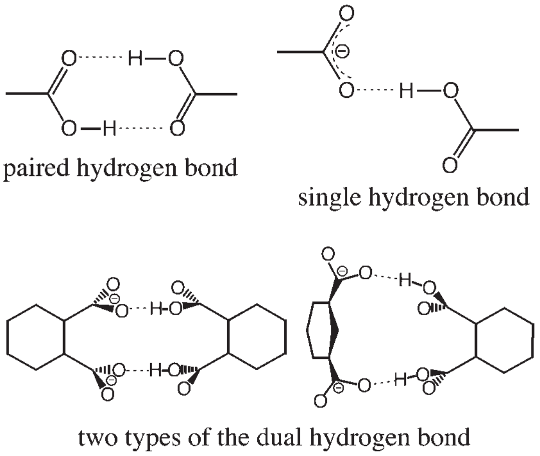

Scheme 3.

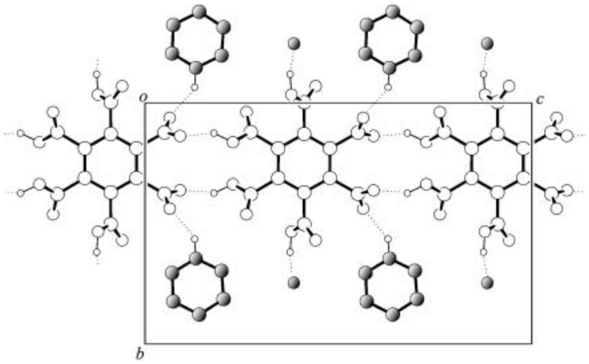

Fig. 10. One-dimensional chain of mellitate ($n = 2$) in $[C_5H_5NH^+]_2\{[C_6(COO)_6H_4]^{2-}\}\cdot 2H_2O$. Fragments with gray spheres are the cations and H_2O.

$\{[C_6(COO)_6H_3]^{3-}\}$ with different deprotonated sites (1,3,5-deprotonation for the 3-methylpyridinium salt and 1,2,3-deprotonation for the piperidinium salt).[39] The other typical sheet was found for the anion with $n = 2$; mellitates arranged in a rhombic mesh with water molecules in the rhombic holes.[39] In all the cases, though the ammonium group acted as a proton-donating group in hydrogen bonds with mellitate, the cations did not interrupt the anion networks and packed between the anion sheets.

3.2.2 One-Dimensional Chain: This structure was observed only for the anion with $n = 2$, and the chain was formed by two pairs of the carboxy–carboxylate single hydrogen bonds (dual hydrogen bond; Scheme 3) between the neighboring mellitates. Therefore, two carboxy and two carboxylate groups participate in the chain formation. Two carboxy groups are always left over, and it can be seen that the carboxy–carboxylate hydrogen bond dominates in hydrogen bonds between mellitates. The proton-accepting crystal solvents (CH_3OH, H_2O, etc.) coordinated to the remaining carboxy groups. As an example, the structure of the pyridinium salt is shown in Fig. 10. The cations coordinated to the carboxylate groups, and were located at peripheries of the chain. In this case, the chain is linear, but zigzag chains were also formed for different cations.[38]

3.2.3 Grid Network with Channel Space: The dual hydrogen bonds between the neighboring mellitates sometimes occur differently. Since the C(ring)–C(carboxy or carboxylate) bond is free for rotation, two pairs of the carboxy–carboxylate single hydrogen bonds occur between mellitates of which the molecular planes are nearly perpendicular (Scheme 3). For $n = 2$, the combination of the above coplanar and this perpendicular types of the dual hydrogen bonds led to the grid network with molecular planes perpendicular to the network plane. As an example, the structure of the 3-methylpyridinium salt is shown in Fig. 11. In this crystal, there are further carboxy–carboxylate hydrogen bonds between the grid networks, forming one-dimensional channels in the network.[38] The cations are accommodated in this channel.

In all of the above cases, mellitate always preferentially forms infinite networks, even when it is combined with cations with hydrogen-bonding ability. Also, there are some connection patterns characteristic of the deprotonation number, and the combination of these patterns leads to the various network structures.

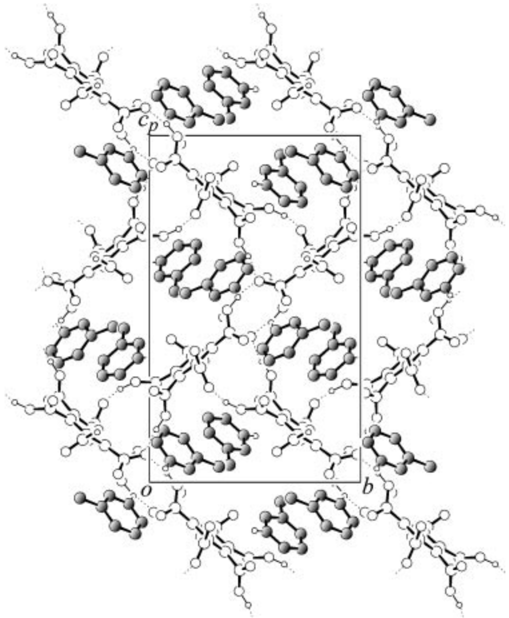

Fig. 11. Grid network of mellitate ($n = 2$) in $[3\text{-}CH_3C_5H_5NH^+]_2\{[C_6(COO)_6H_4]^{2-}\}$. Fragments with gray spheres are the cations.

3.3 Mellitate Salts with π-Radical Cations. From the above study, it became clear that mellitate had excellent ability to form self-organized networks. Since there are several strong carboxy–carboxylate hydrogen bonds between the anions, the self-assembling energy is thought to be rather large. If one combined this component with π-radical cations, the radicals could not take their preferred arrangement and would be packed in the space provided by the mellitate networks. In this way, one could create novel π-radical arrangements, and this possibility was examined by combining with radical cations of the TTF derivatives. A conventional electrochemical technique of crystal growth with mellitic acid and pyridine derivatives as electrolytes was found to give several radical cation salts.[2,40] The following is a description about some of the crystals, mainly concerned with the anion networks.

Mellitate in the EDT-TTF (ethylenedithiatetrathiafulvalene) and TMTTF (tetramethyltetrathiafulvalene) salts forms a two-dimensional sheet. Mellitate with $n = 2$ in the EDT-TTF salt first forms a one-dimensional chain along the a axis as described in **3.2.2**. Then, two carboxy groups that do not participate in the chain formation form hydrogen bonds with mellitate in the neighboring chains, forming a two-dimensional sheet (Fig. 12a). Since hydrogen-bonding functional groups are absent in EDT-TTF, it becomes possible to form hydrogen bonds between the mellitate one-dimensional chains. EDT-TTF forms one-dimensional columns along the [210] and [2−10] directions with weak interactions with neighboring columns in the space between the anion sheets. Since EDT-TTF was in the partially oxidized state, $[\mathrm{EDTTTF}^{x+}]_3\{[C_6(COO)_6H_4]^{2-}\}$ with $x = 2/3$, relatively high conductivity was observed; $10\ \mathrm{S\,cm^{-1}}$ at room temperature. However, the temperature dependence was semiconducting due to the three-fold periodicity along the column direction.

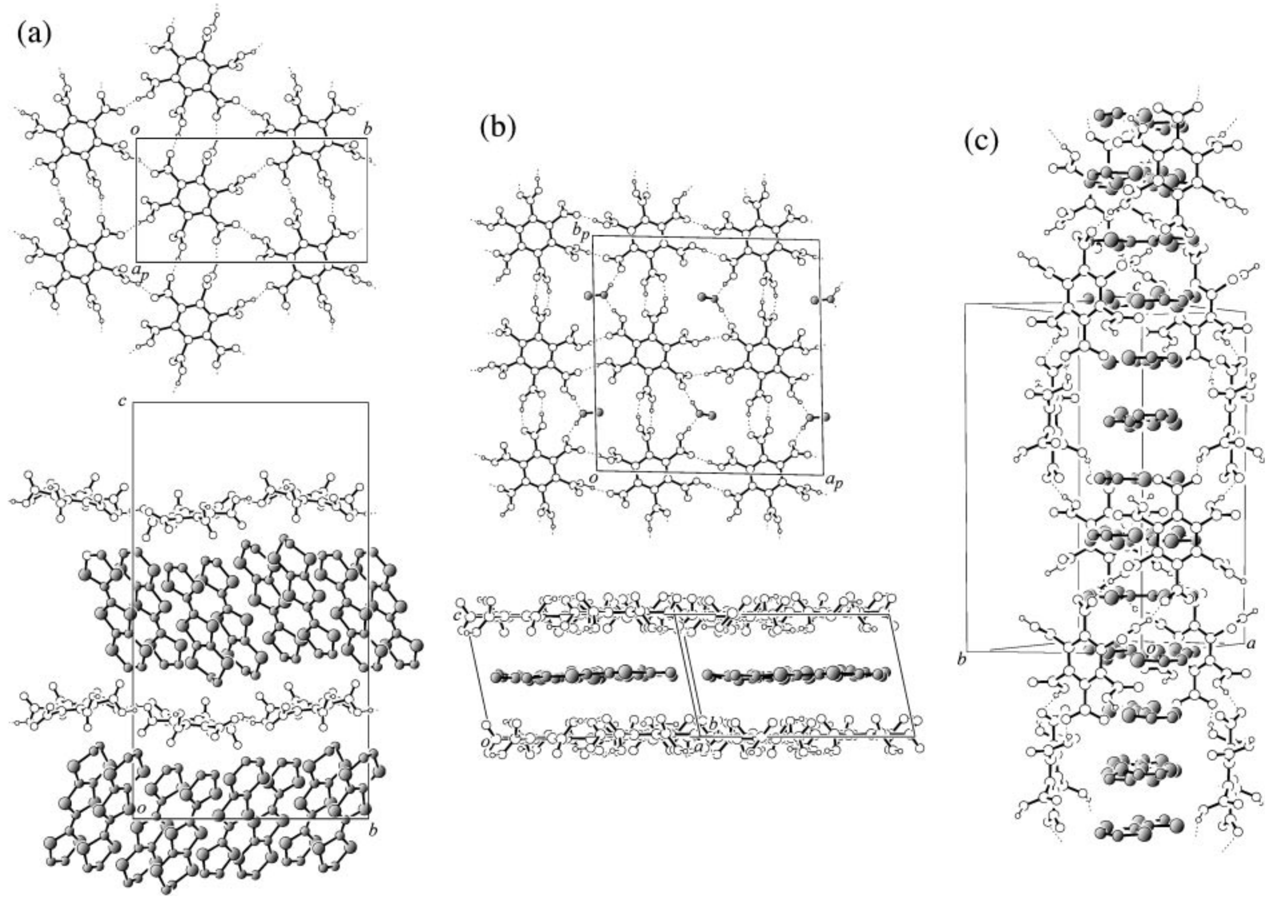

Fig. 12. Crystal structures of the π-radical cation salts of mellitate. (a) Mellitate network and the EDT-TTF packing in $[\mathrm{EDTTTF}^{x+}]_3\{[C_6(COO)_6H_4]^{2-}\}$ with $x = 2/3$. (b) Mellitate network and the TMTTF packing in $[\mathrm{TMTTF}^{+}]$-$\{[C_6(COO)_6H_5]^{-}\}\cdot CH_3OH$. (c) Double helix network of mellitate and the helical TTF column in $[\mathrm{TTF}^{+}]_2\{[C_6(COO)_6H_4]^{2-}\}$. Fragments with gray spheres are the π-radical cations and CH_3OH in (b).

In the TMTTF salt with the composition of $[\mathrm{TMTTF}^{+}]$-$\{[C_6(COO)_6H_5]^{-}\}\cdot CH_3OH$, the deprotonation number was 1. If an anion with $n = 1$ bound with another anion by the dual hydrogen bond, only an isolated dimer would be formed. In this salt, a carboxy–carboxy single hydrogen bond newly participates in the one-dimensional chain formation along the *a* axis. Furthermore, due to insufficient number of carboxylate groups, paired hydrogen bonds are formed between the carboxy groups that do not participate in the chain formation. Consequently, the chains are connected to form a two-dimensional sheet (Fig. 12b). In such sheets, there are rather large voids, and they are occupied by CH_3OH. The TMTTF radical cations are packed between the anion sheets. The most characteristic feature in this structure is that there are no π–π overlaps between the cations; their molecular planes are parallel to the anion sheet. This is thought to because the mellitate network formation surpasses the π–π interactions between π-radicals, and supports the possibility of controlling π-radical arrangement by mellitate networks.

A further unique structure was observed in the TTF salt.[41] The composition is $[\mathrm{TTF}^{+}]_2\{[C_6(COO)_6H_4]^{2-}\}$, and mellitate with $n = 2$ constructs the network. The neighboring mellitates are connected by the dual hydrogen bonds, forming a one-dimensional chain similar to that shown in **3.2.2**. However, in this salt, each single mellitate is doubly involved in two different chains. Furthermore, each chain does not extend along the direction parallel to the molecular plane but extends helically. The two chains intertwine and form a double helix (Fig. 12c). The double helix units arrange in a hexagonal manner, and provide a one-dimensional channel space. In this one-dimensional space, the TTF radical cations are accommodated. Since the central axis of the TTF column coincides with a screw axis, the one-dimensional column is subjected to twisting distortion. Close inspection indicated that the TTF radical cations were alternately disordered, and that dimerizing distortion occurs in two different phases. There must be a kink at the boundary of these two phases, and this could behave as a soliton.

4. Conclusion

In the above sections, our approaches to the control of molecular arrangements for mainly π-radicals have been described. The relative arrangements of π-radicals are important for electronic functionalities of the crystals. In the previous studies, material designs were performed while keeping the preferable arrangement for π-radicals. Our approach is rather the opposite, and we have intended to frustrate the π–π interactions. By this strategy, two-dimensional π–π stacking structure of phthalocyanines, which has not been realized previously, has become possible, and the novel helical TTF column has been realized by packing TTF in the space provided by a network formed by counter-ions. The π–π stacking of π-radicals itself can be regarded as a kind of supramolecular formation, and introduction of interactions that can compete with the π–π interaction may be a promising approach to the design of π-radical arrangements.

The experimental results introduced in this paper have been obtained by many graduates and students in the laboratory of solid-state chemistry at the Division of Chemistry, Graduate School of Science, Hokkaido University. The author would like to express his sincere thanks to them for their efforts, unexpected ideas, and careful and patient experiments. Also, these achievements were not attained without the help and cooperation of the staff members of the laboratory and collaborators in many places in Japan, and the author deeply thanks them. These works were supported in part by Grants-in-Aid for Scientific Research from the Ministry of Education, Culture, Sports, Science and Technology of the Japanese Government and Grants-in-Aid for Scientific Research from the Japan Society for the Promotion of Science.

References

1 T. Inabe and H. Tajima, *Chem. Rev.*, **104**, 5503 (2004), and references therein.

2 T. Inabe, *J. Mater. Chem.*, **15**, (2005), DOI: 10.1039/b413848a.

3 T. J. Marks, *Angew. Chem., Int. Ed. Engl.*, **29**, 857 (1990), and references therein.

4 D. Jérome, A. Mazaud, M. Ribault, and K. Bechgaard, *J. Phys., Lett.*, **41**, L95 (1980); D. Jérome, *Chem. Rev.*, **104**, 5565 (2004).

5 R. P. Shibaeva and E. B. Yagubskii, *Chem. Rev.*, **104**, 5347 (2004); T. Ishiguro, K. Yamaji, and G. Saito, "Organic Superconductors," 2nd ed, Springer-Verlag, New York (1998); J. M. Williams, J. R. Ferraro, R. J. Thorn, K. D. Carlson, U. Geiser, H. H. Wang, A. M. Kim, and M.-H. Wangbo, "Organic Superconductors (Including Fullerenes). Synthesis, Structure, Properties, and Theory," Prentice Hall, Englewood Cliffs, NJ (1992).

6 W. J. Pietro, T. J. Marks, and M. A. Ratner, *J. Am. Chem. Soc.*, **107**, 5387 (1985).

7 B. N. Diel, T. Inabe, N. K. Jaggi, J. W. Lyding, O. Schneider, M. Hanack, C. R. Kannewurf, T. J. Marks, and L. H. Schwartz, *J. Am. Chem. Soc.*, **106**, 3207 (1984).

8 D. C. Weber, P. Brant, R. S. Nohr, S. G. Haupt, and K. J. Wynne, *J. Phys., Colloq.*, **C3**, 639 (1983).

9 Y. Orihashi, N. Kobayashi, E. Tsuchida, H. Matsuda, H. Nakanishi, and M. Kato, *Chem. Lett.*, **1985**, 1617.

10 J. Metz and M. Hanack, *J. Am. Chem. Soc.*, **105**, 828 (1983).

11 T. Inabe and Y. Maruyama, *Chem. Lett.*, **1989**, 55.

12 K. Morimoto and T. Inabe, *J. Mater. Chem.*, **5**, 1749 (1995).

13 A. Fujita, H. Hasegawa, T. Naito, and T. Inabe, *J. Porphyrins Phthalocyanines*, **3**, 720 (1999).

14 P. Turek, J. J. Andre, and J. Simon, *Solid State Commun.*, **63**, 741 (1987); P. Turek, M. Moussavi, P. Petit, and J. J. Andre, *Synth. Met.*, **29**, F65 (1989); M. Dumm, P. Lunkenheimaer, A. Loidl, B. Assmann, H. Homborg, and P. Fulde, *J. Chem. Phys.*, **104**, 5048 (1996); M. Dumm, R. Spitzfaden, P. Lunkenheimer, M. Dressel, A. Loidl, B. Assmann, H. Homborg, and P. Fulde, *Synth. Met.*, **84**, 925 (1997).

15 P. Pitet, K. Holczer, and J. J. Andre, *J. Phys.*, **48**, 1363 (1987); P. Petit and J. J. Andre, *J. Phys. Fr.*, **49**, 2059 (1988); J. J. Andre, K. Holczer, P. Petit, M. T. Riou, C. Clariss, R. Even, M. Fourmigue, and J. Simon, *Chem. Phys. Lett.*, **115**, 463 (1985).

16 H. Sugimoto, M. Mori, H. Masuda, and T. Taga, *J. Chem. Soc., Chem. Commun.*, **1986**, 962.

17 N. Matsumura, A. Fujita, T. Naito, and T. Inabe, *J. Mater. Chem.*, **10**, 2266 (2000).

18 T. Naito, N. Matsumura, and T. Inabe, *J. Porphyrins Phthalocyanines*, **8**, 1258 (2004).

19 H. Hasegawa, T. Naito, T. Inabe, T. Akutagawa, and T. Nakamura, *J. Mater. Chem.*, **8**, 1567 (1998).

20 T. Inabe, T. Asari, H. Hasegawa, M. Matsuda, E. H. Gacho, N. Matsumura, K. Takeda, and T. Naito, *Synth. Met.*, **133–134**, 515 (2003).

21 M. Matsuda, T. Naito, T. Inabe, N. Hanasaki, and H. Tajima, *J. Mater. Chem.*, **11**, 2493 (2001).

22 K. Mitsuya, T. Inabe, T. Okuno, and K. Awaga, *Mol. Cryst. Liq. Cryst.*, **296**, 293 (1997).

23 H. Hasegawa, S. Takano, N. Miyajima, and T. Inabe, *Mol. Cryst. Liq. Cryst.*, **285**, 113 (1996).

24 S. Takano, T. Naito, and T. Inabe, *J. Mater. Chem.*, **8**, 511 (1998).

25 G. Saito and J. P. Ferraris, *Bull. Chem. Soc. Jpn.*, **53**, 2141 (1980); J. B. Torrance, *Acc. Chem. Res.*, **12**, 79 (1979).

26 S. Takano, T. Naito, and T. Inabe, *Chem. Lett.*, **1998**, 1249.

27 T. Asari, T. Naito, T. Inabe, T. Matsuda, and H. Tajima, *Chem. Lett.*, **33**, 128 (2004).

28 M. Matsuda, T. Naito, T. Inabe, N. Hanasaki, H. Tajima, T. Otsuka, K. Awaga, B. Narymbetov, and H. Kobayashi, *J. Mater. Chem.*, **10**, 631 (2000).

29 M. Matsuda, T. Asari, T. Naito, T. Inabe, N. Hanasaki, and H. Tajima, *Bull. Chem. Soc. Jpn.*, **76**, 1935 (2003).

30 N. Hanasaki, H. Tajima, M. Matsuda, T. Naito, and T. Inabe, *Phys. Rev. B*, **62**, 5839 (2000).

31 N. Hanasaki, M. Matsuda, H. Tajima, T. Naito, and T. Inabe, *J. Phys. Soc. Jpn.*, **72**, 3226 (2003).

32 N. Hoshino, T. Inabe, T. Mitani, and Y. Maruyama, *Bull. Chem. Soc. Jpn.*, **61**, 4207 (1988).

33 T. Inabe, N. Hoshino, T. Mitani, and Y. Maruyama, *Bull. Chem. Soc. Jpn.*, **62**, 2245 (1989).

34 T. Inabe, I. Gautier-Luneau, N. Hoshino, K. Okaniwa, H. Okamoto, T. Mitani, U. Nagashima, and Y. Maruyama, *Bull. Chem. Soc. Jpn.*, **64**, 801 (1991).

35 T. Inabe, I. Luneau, T. Mitani, Y. Maruyama, and S. Takeda, *Bull. Chem. Soc. Jpn.*, **67**, 612 (1994).

36 T. Inabe, N. Hoshino-Miyajima, I. Luneau, T. Mitani, and Y. Maruyama, *Bull. Chem. Soc. Jpn.*, **67**, 622 (1994).

37 T. Inabe, *New J. Chem.*, **15**, 129 (1991).

38 N. Kobayashi, T. Naito, and T. Inabe, *Bull. Chem. Soc. Jpn.*, **76**, 1351 (2003).

39 N. Kobayashi, T. Naito, and T. Inabe, *CrystEngComm.*, **6**, 189 (2004).

40 T. Inabe, N. Kobayashi, and T. Naito, *J. Phys. IV France*, **114**, 449 (2004).

41 N. Kobayashi, T. Naito, and T. Inabe, *Adv. Mater.*, **16**, 1803 (2004).

Tamotsu Inabe was born in 1954 in Hokkaido. He received his B.Sc. degree in 1976 and Ph.D. degree in 1981 from Hokkaido University in the field of solid-state chemistry of molecular materials (Professor Yoshio Matsunaga). Then, he worked as a postdoctoral fellow with Professor Tobin J. Marks at Northwestern University, U. S. A. In 1984, he was appointed as a research associate at Institute for Molecular Science, Okazaki. He was promoted to an associate professor of the Department of Chemistry, Faculty of Science, Hokkaido University in 1992, and became a full professor in 1993. New materials design is the most important subject in his research.